Electronic Supplementary Material (ESI) for Analyst.

Tunable Graphene Oxide for Low-Fouling Electrochemical Sensing of UA in Human Serum

Gang Li [a], Chunying Xu [a, *], Hui Xu [b], Liju Gan [a], Kai Sun [c], Baiqing Yuan [a, *]

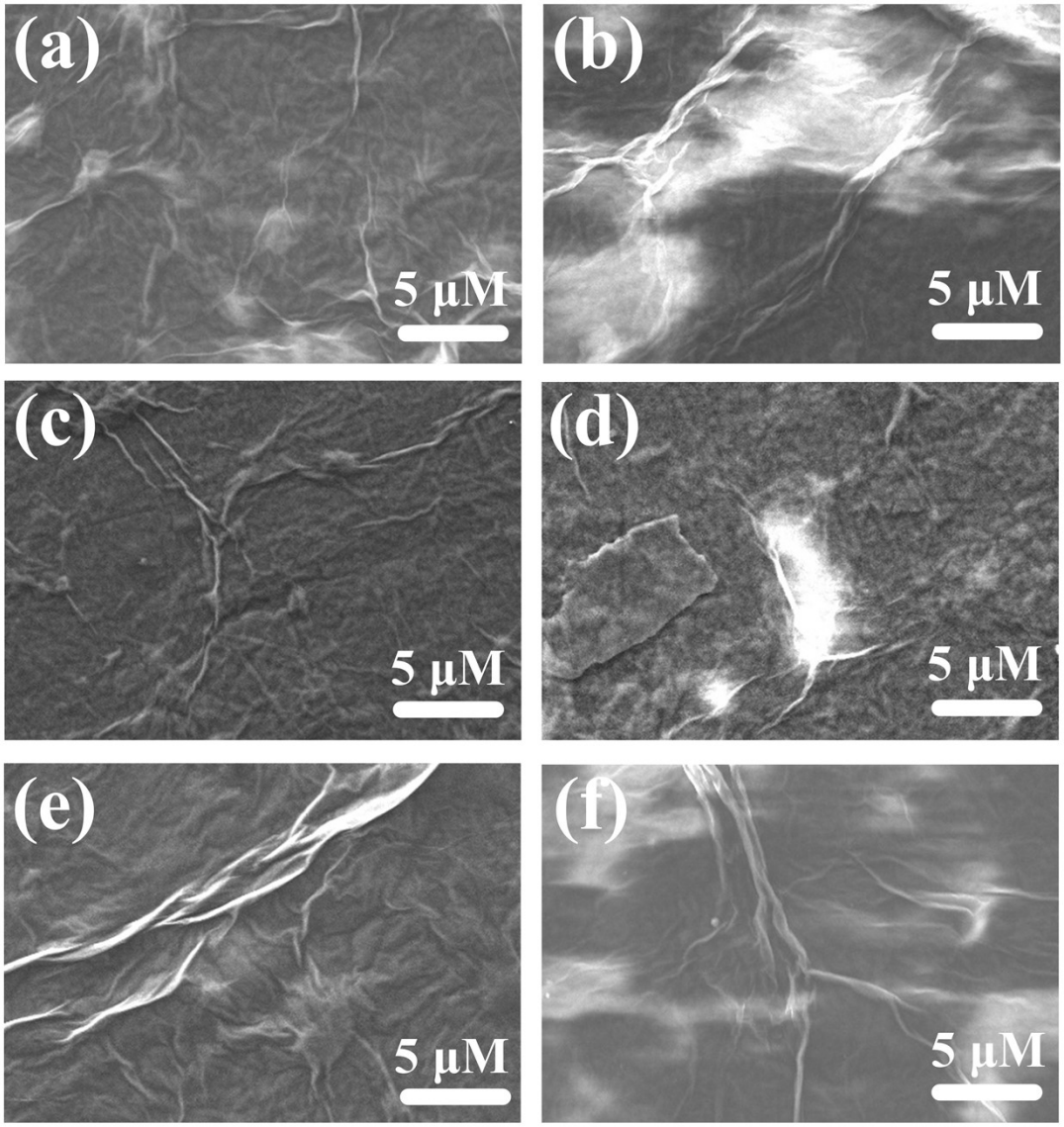

Fig. S-1 SEM images of (a) GO/GCE, (b) GO-BSA/GCE, (c) $GO_{-0.75}$/GCE, (d) $GO_{-0.75}$-BSA/GCE, (e) EHGO/GCE, and (f) EHGO-BSA/GCE.

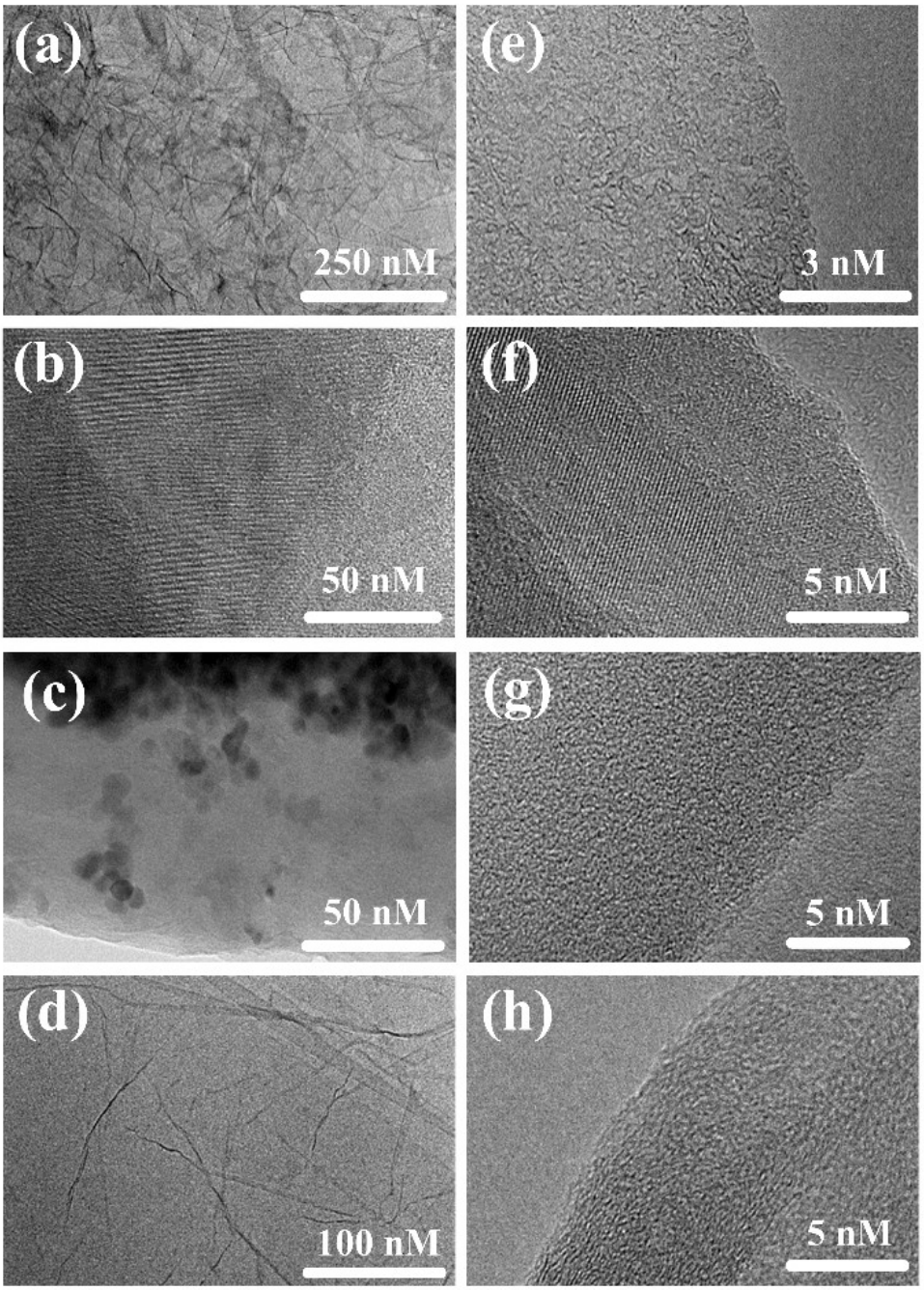

Fig. S-2 TEM and HRTEM images of (a, e) GO/GCE, (b, f) GO-BSA/GCE, (c, g) $GO_{-0.75}$/GCE, (d, h) EHGO/GCE.

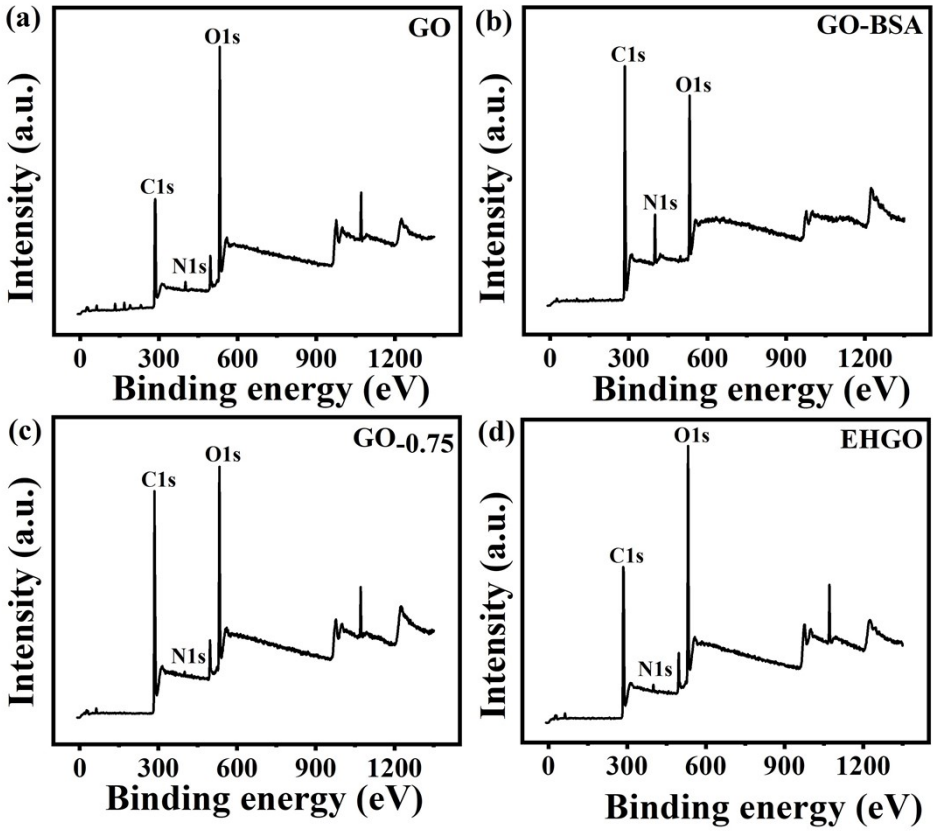

Fig. S-3 XPS survey spectrum of (a) GO, (b) GO-BSA, (c) $GO_{-0.75}$, (d) EHGO.

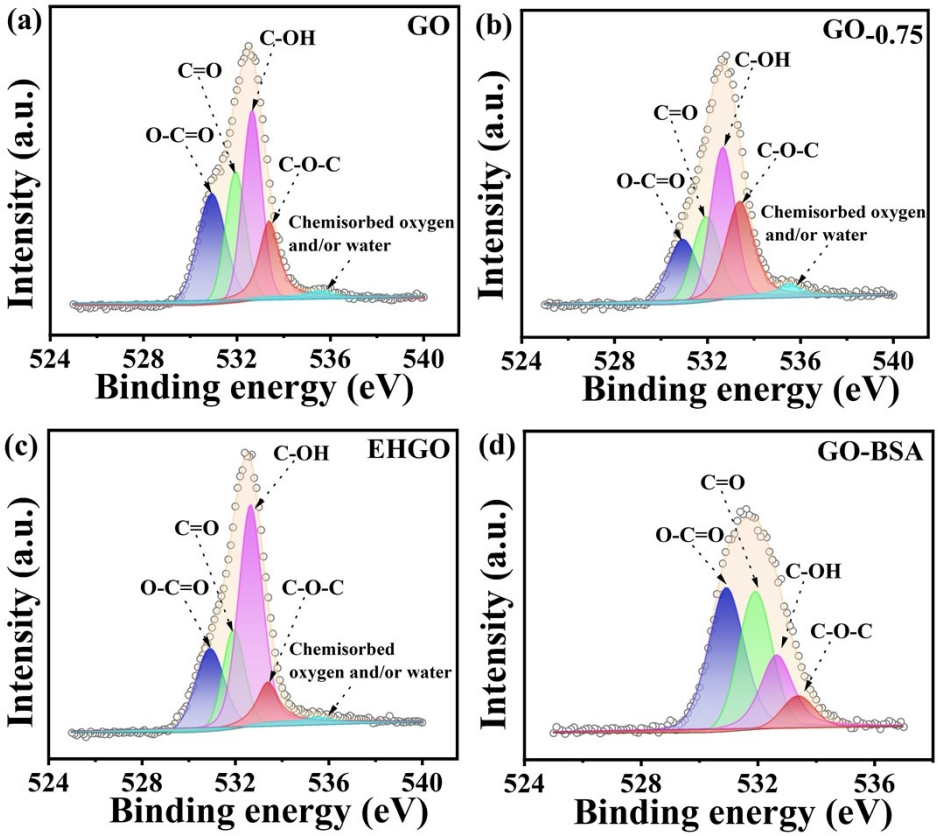

Fig. S-4 O1s XPS spectra of (a) GO, (b) $GO_{-0.75}$, (c) EHGO, (e) GO-BSA.

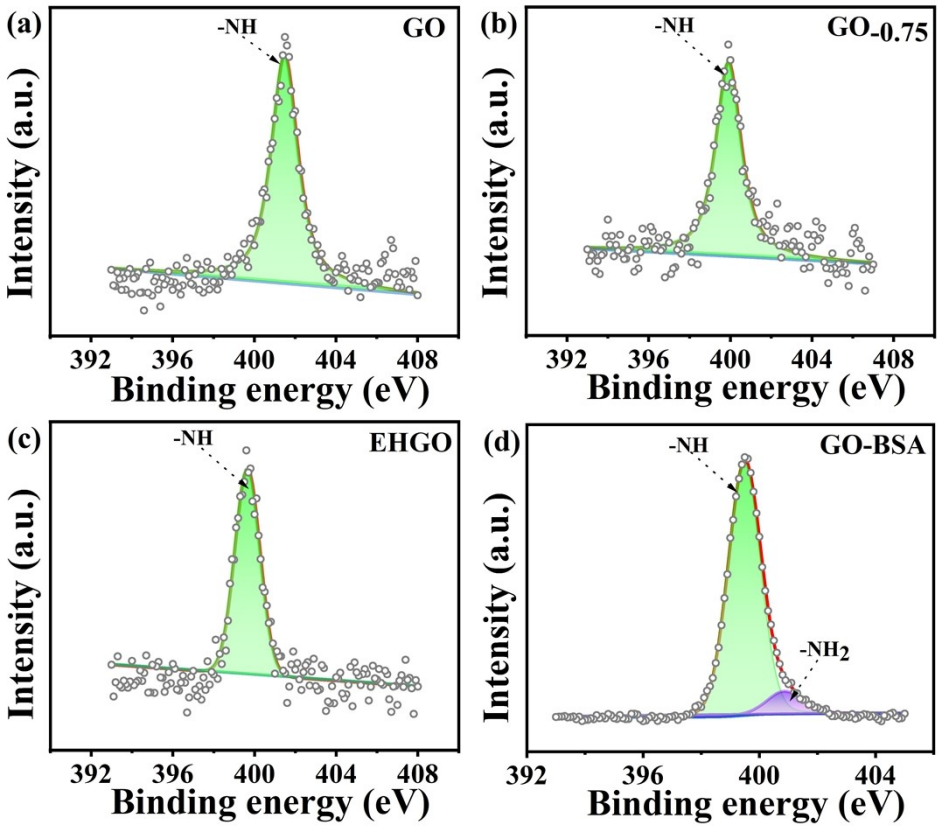

Fig. S-5 N1s XPS spectra of (a) GO, (b) $GO_{-0.75}$, (c) EHGO, (e) GO-BSA.

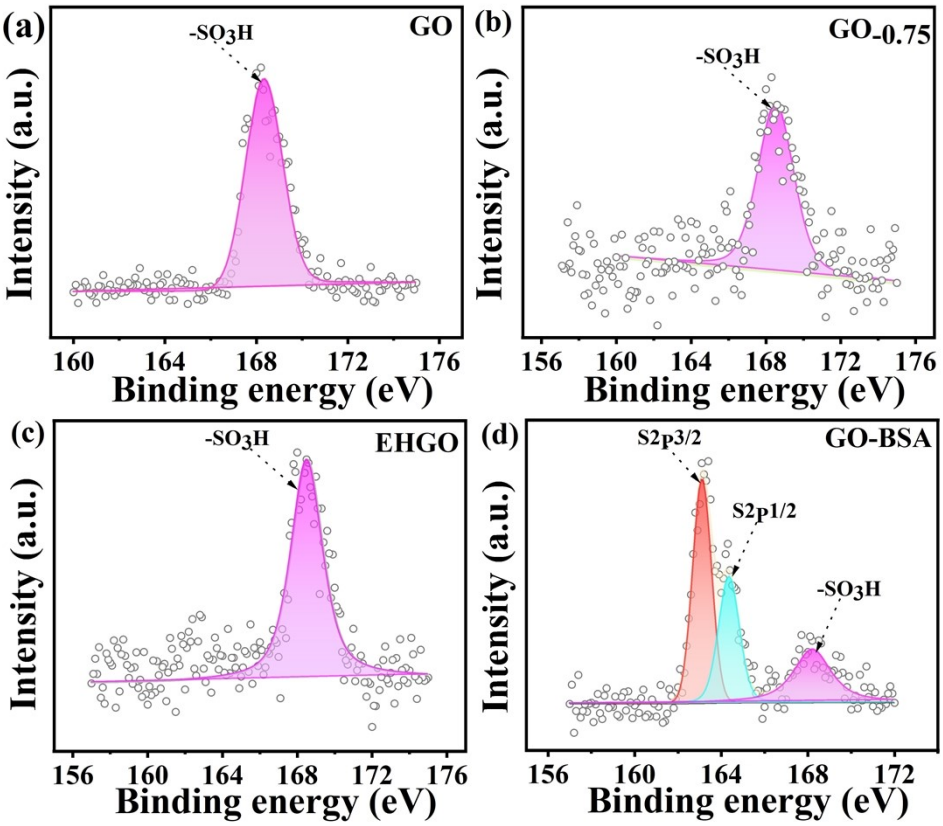

Fig. S-6 S2p XPS spectra of (a) GO, (b) $GO_{-0.75}$, (c) EHGO, (e) GO-BSA.

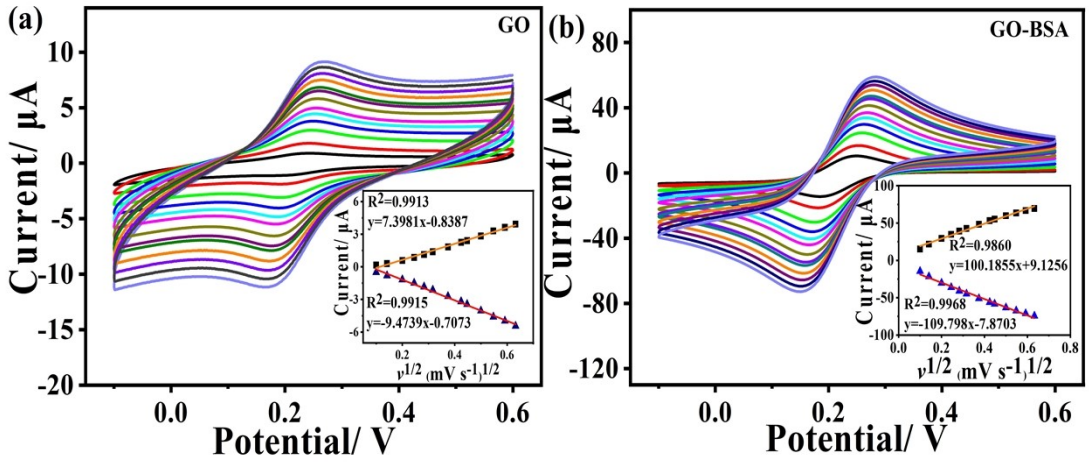

Fig. S-7 CVs of GO/GCE and GO-BSA/GCE in 0.1 M KCl solution in the presence of 5 mM $K_3Fe(CN)_6$ at different scan rates. Inset: the linear plot of anodic and cathodic peak currents versus the square root of scan rate.

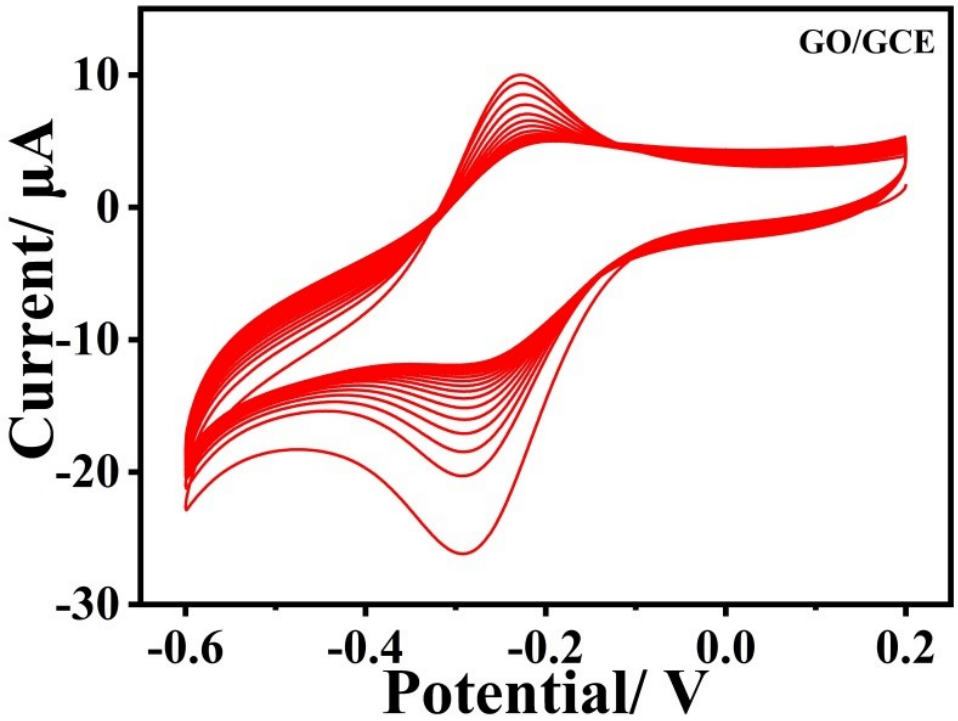

Fig. S-8 CVs of GO/GCE in 0.1 M PBS (pH = 7.0) at a scan rate of 25 mV s^{-1} for 30 cycles after scanning in 5 mM $Ru(NH_3)_6Cl_3$.

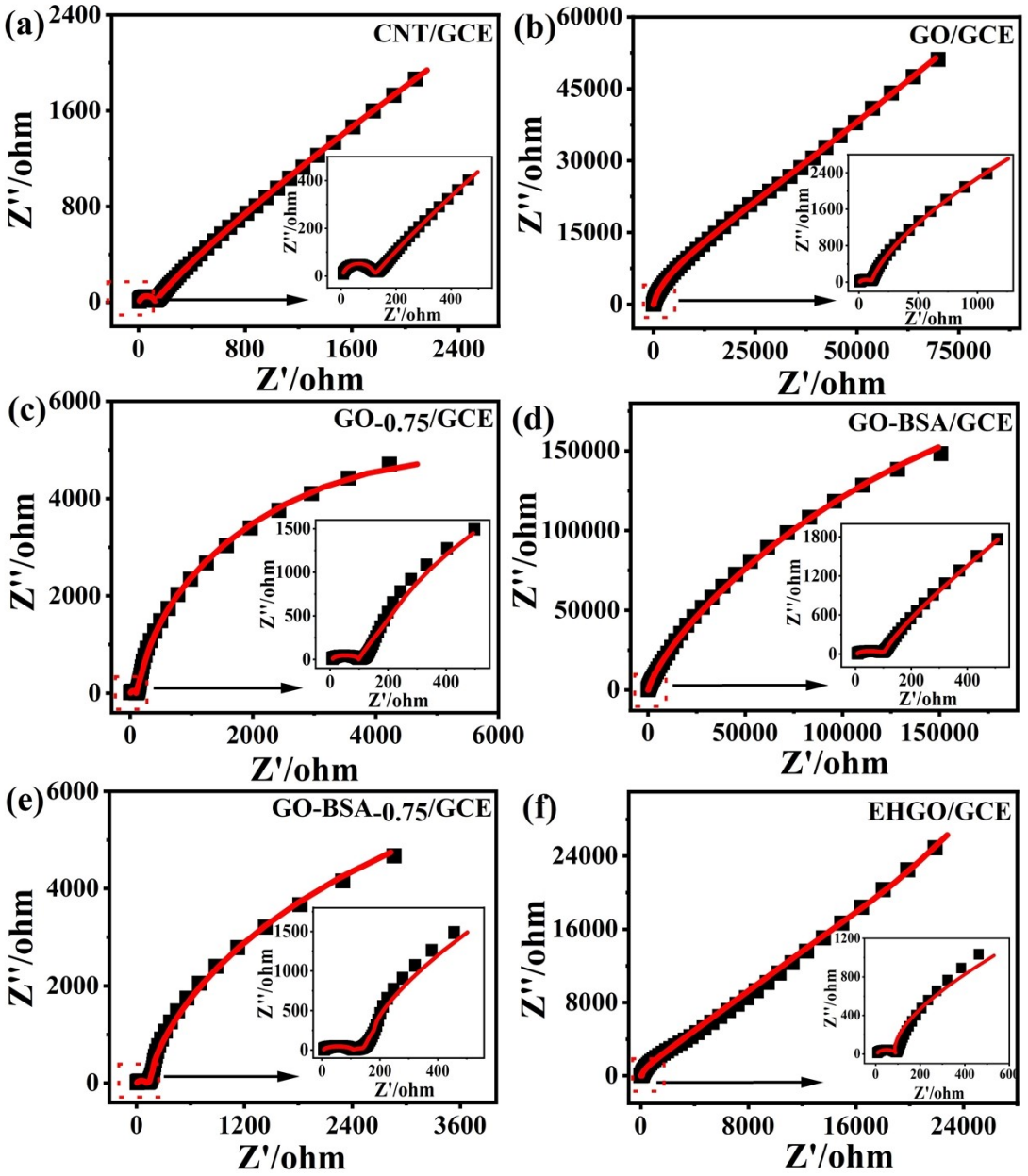

Fig. S-9 Nyquist diagrams for (a) CNT/GCE, (b) GO/GCE, (c) $GO_{-0.75}$/GCE, (d) GO-BSA/GCE, (e) $GO\text{-}BSA_{-0.75}$/GCE, (f) EHGO/GCE in 0.1 M KCl solution in the presence of 5 mM $K_3Fe(CN)_6$. The symbols and solid lines present the experimental and the fitted data, respectively. Inset: The amplified Nyquist diagrams. The frequency range of EIS was from 1 MHz to 0.1 Hz at 0.25V.

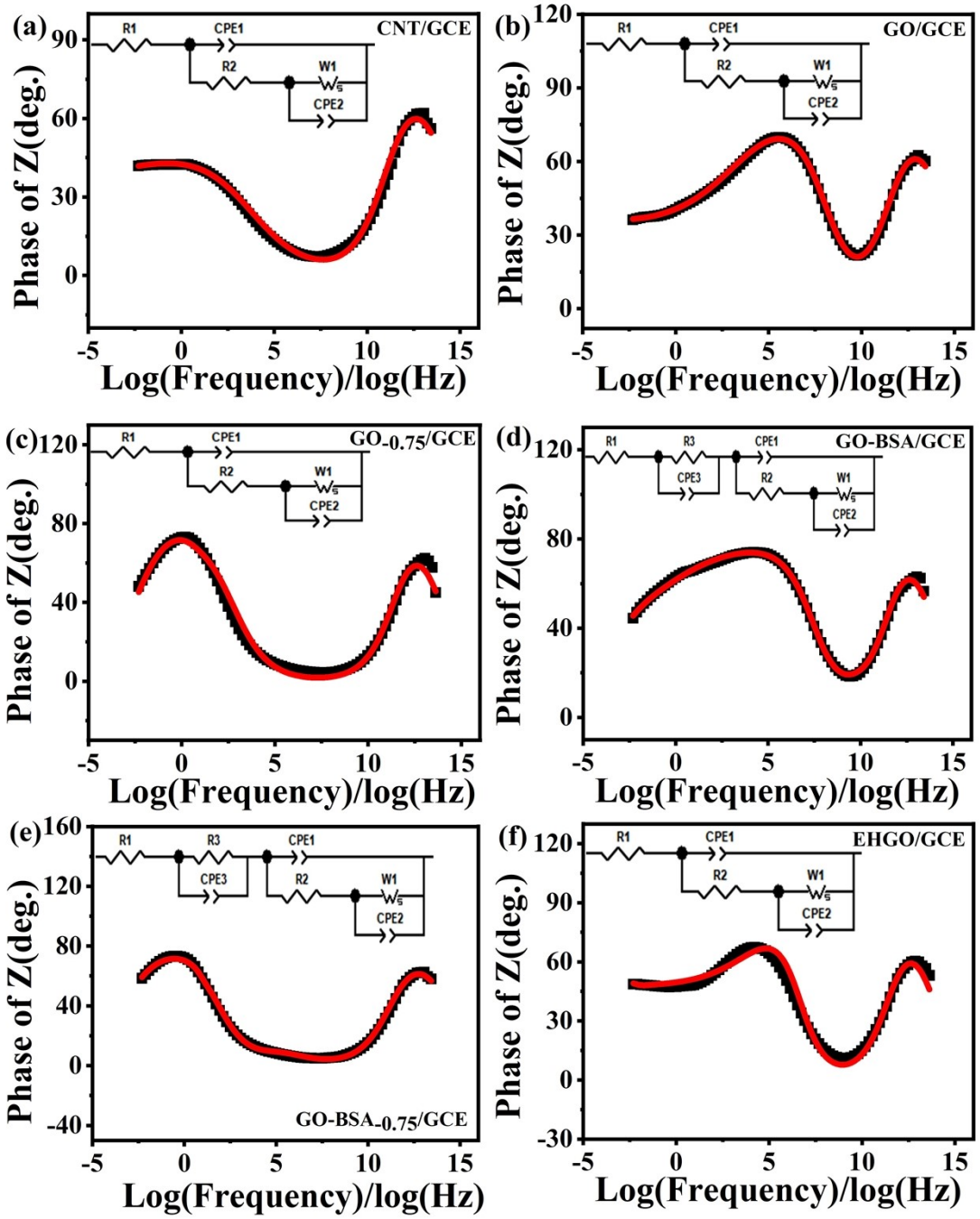

Fig. S-10 Phase angle diagrams vs log of frequency of Bode plots for (a) CNT/GCE, (b) GO/GCE, (c) $GO_{-0.75}$/GCE, (d) GO-BSA/GCE, (e) $GO\text{-}BSA_{-0.75}$/GCE, (f) EHGO/GCE. Inset: The electrical equivalent circuit.

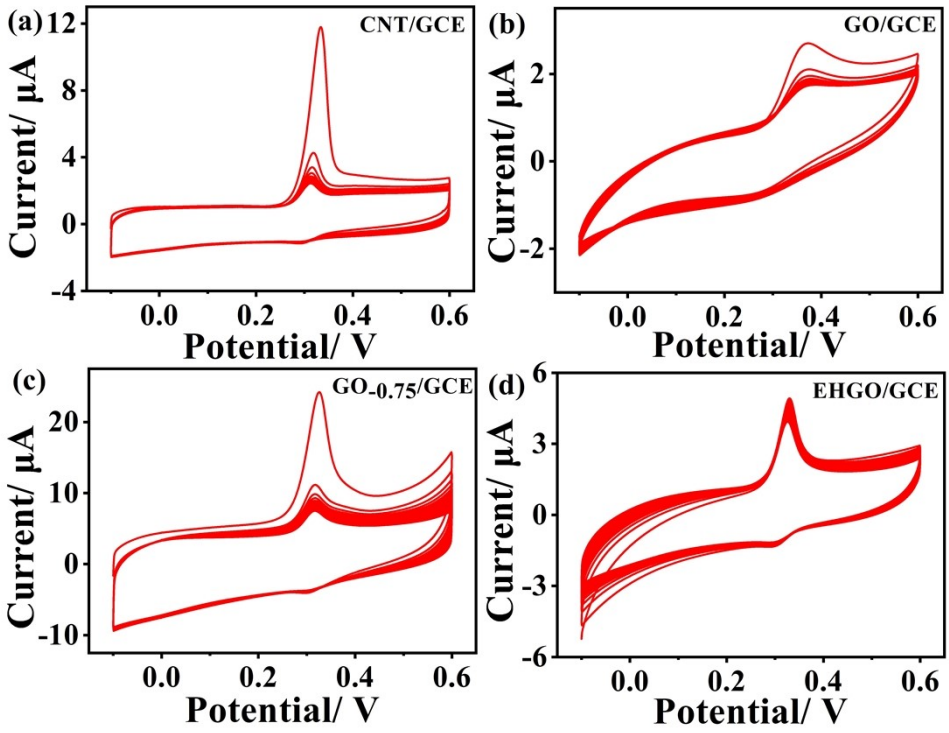

Fig. S-11 CVs of (a) CNT/GCE, (b) GO/GCE, (c) $GO_{-0.75}$/GCE, (d) EHGO/GCE in 0.1 M PBS (pH = 7.0) containing 100 μM UA for 30 cycles at a scan rate of 25 mV s^{-1}.

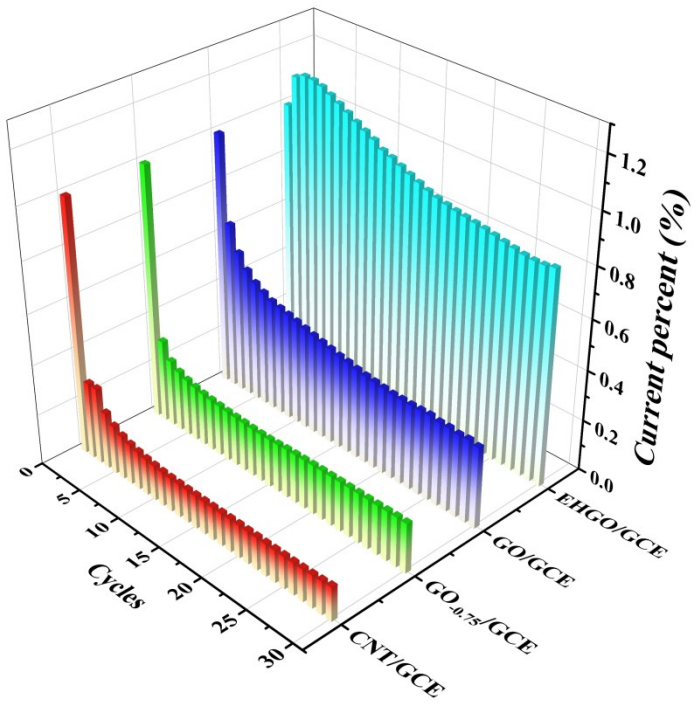

Fig. S-12 Normalized CV peak current percent of CNT/GCE, GO/GCE, $GO_{-0.75}$/GCE, and EHGO/GCE in 0.1 M PBS (pH = 7.0) containing 100 μM UA.

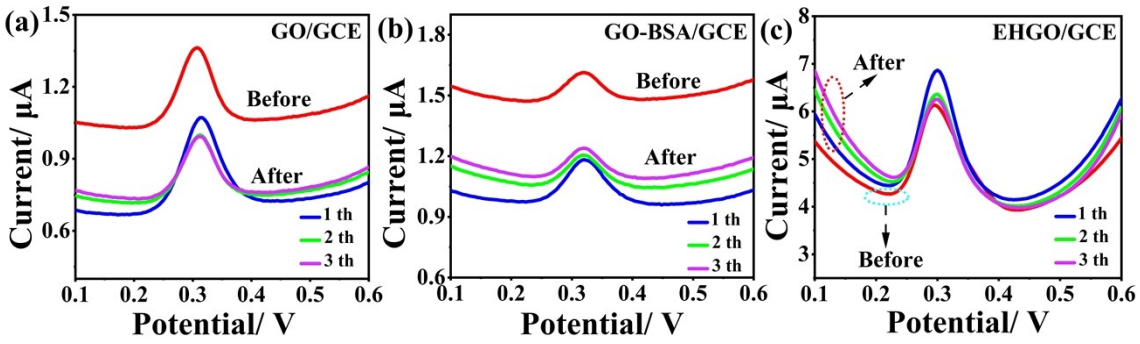

Fig. S-13 DPV responses of 10 μM UA at (a) GO/GCE, (b) GO-BSA/GCE, and (c) EHGO/GCE before and after immersion in undiluted serum for 1 hour.

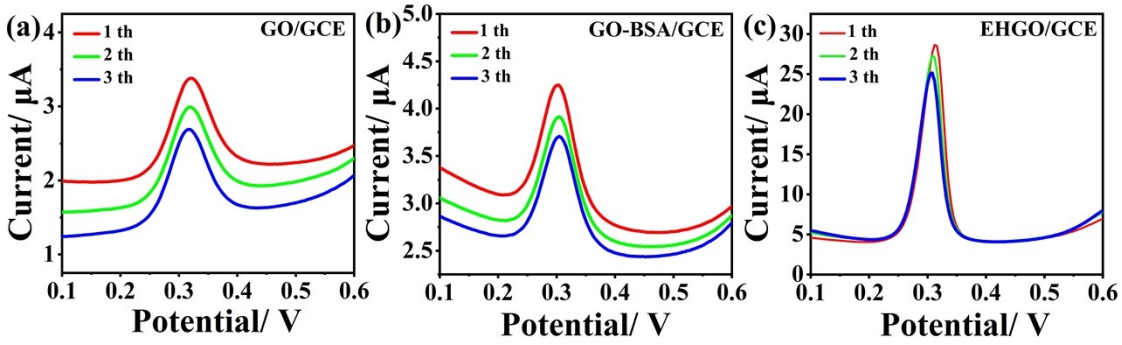

Fig. S-14 Successive DPV responses of (a) GO/GCE, (b) GO/GCE, (c) EHGO/GCE in diluted human serum in 0.1 M PBS (pH=7.0). The human serum was diluted two times.

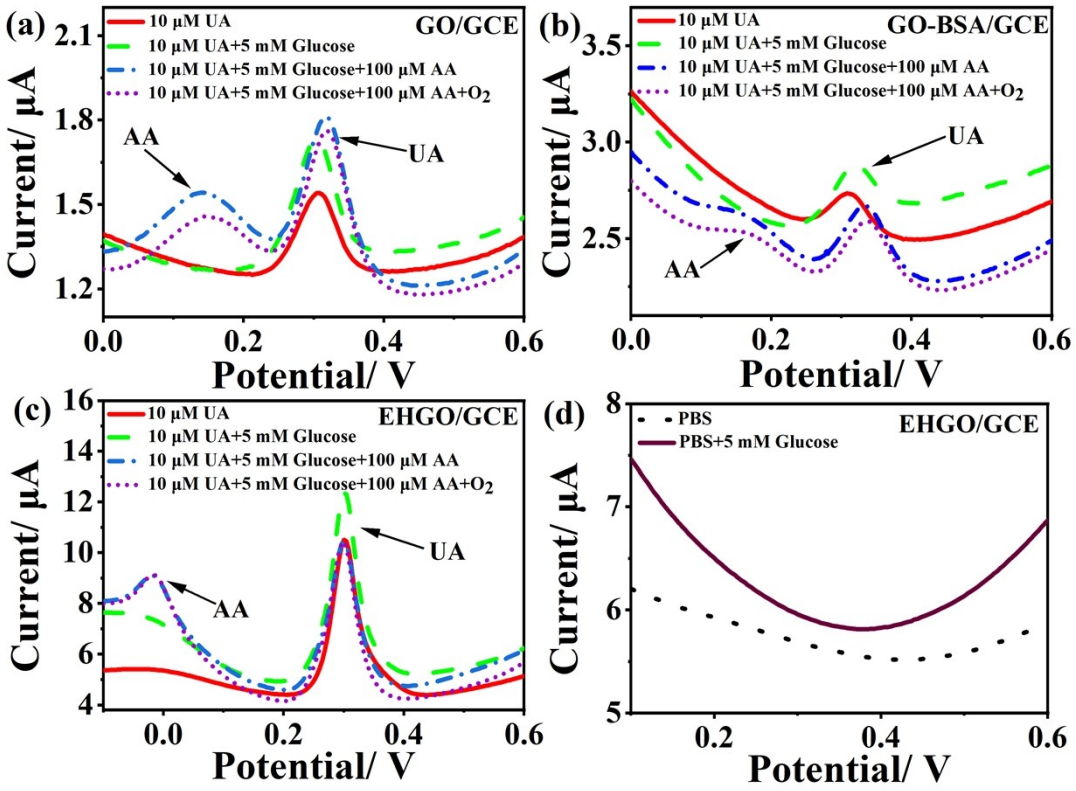

Fig. S-15 DPV responses of (a) GO/GCE, (b) GO-BSA/GCE, and (c) EHGO/GCE in 0.1 M PBS (pH = 7.0) with 10 μM UA in the presence of 5 mM glucose, 100 μM AA, and saturated O_2. (d) DPV responses of EHGO/GCE in the absence (dotted line) and presence (solid line) of 5 mM glucose.

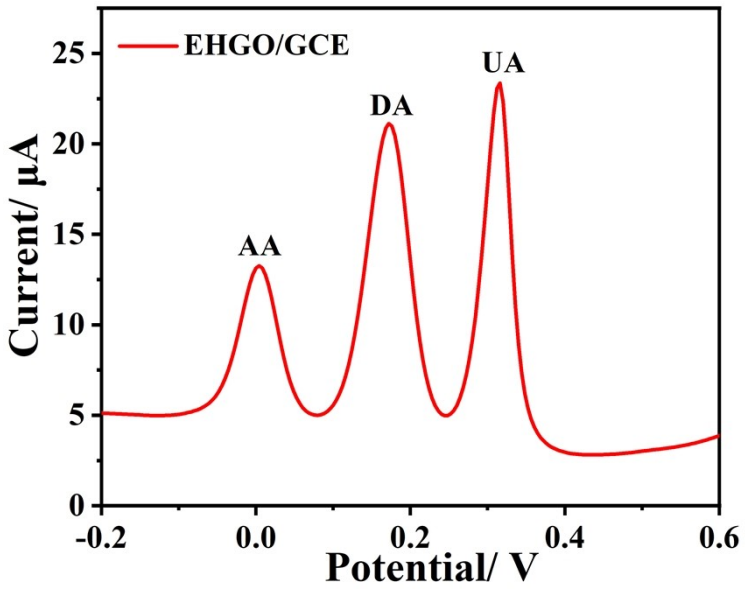

Fig. S-16 DPV response of EHGO/GCE in the presence of 500 μM AA, 10 μM DA, and 20 μM UA in 0.1 M PBS (pH = 7.0).

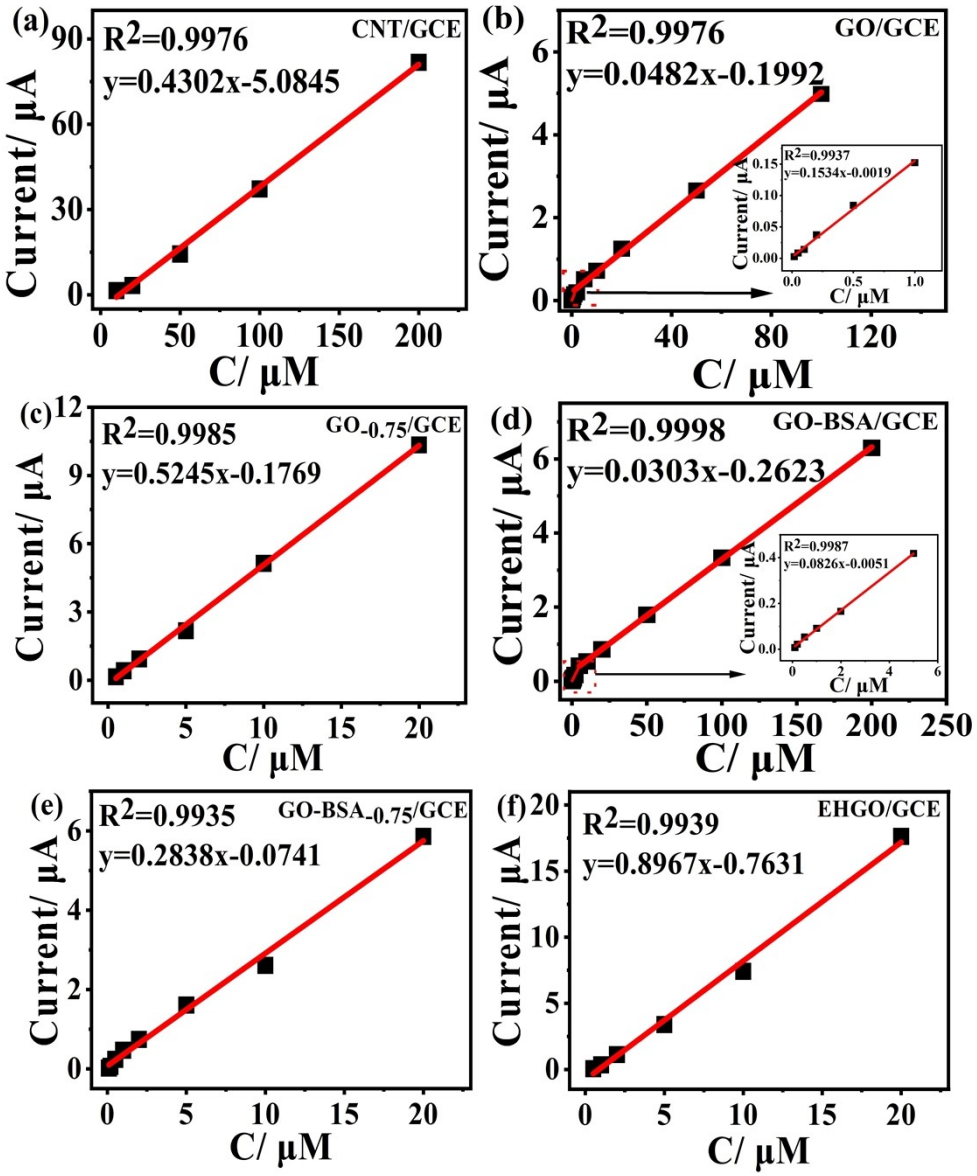

Fig. S-17 The corresponding linear calibration plot of peak current versus concentration of UA. Inset: The amplified linear calibration plot.

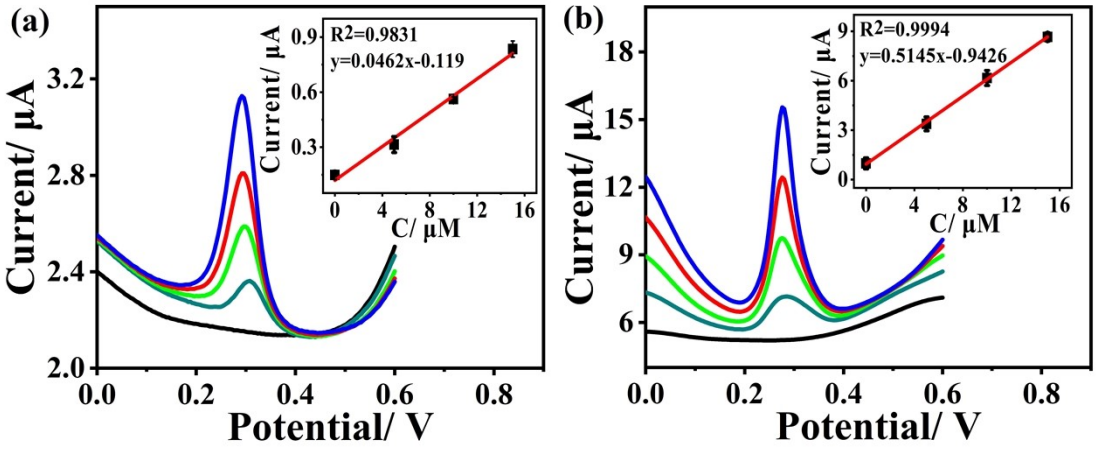

Fig. S-18 DPV curves of the (a) GO/GCE and (b) EHGO/GCE for different concentrations of UA (From bottom to top: 0; 5; 10; 15 μM) spiked in diluted human serum in 0.1 M PBS (pH=7.0). Inset: The corresponding calibration curves and error bars. (The human serum was diluted 50-fold.)

Table S-1 Fitted parameters for C1s XPS spectra.

Materials	Parameters	C1s					
		C=C	**C-C**	**C-S**	**C-O**	**C=O**	**O-C=O**
GO	Position (eV)	284.66	285.1		286.84	288.0	288.95
	Area	21391	3112		23703	2982	1457
	percentage	40.6	5.9		45.0	5.7	2.8
EHGO	Position (eV)	284.63	285.2		286.76	288.0	288.95
	Area	38399	1723		34091	4031	1895
	percentage	47.9	2.2		42.5	5.0	2.4
$GO_{-0.75}$	Position (eV)	284.62	285.15		286.78	288.0	288.95
	Area	38027	3171		27911	1349	2423
	percentage	52.2	4.4		38.3	1.9	3.2
GO-BSA	Position (eV)	284.33	285.36	286.01	286.95	287.84	288.91 (O-C=O/-CO-NH-)
	Area	40725	6769	6861	6993	4862	1235
	percentage	60.4	10.0	10.2	10.4	7.2	1.8

Table S-2 The C/O ratio for C1s XPS spectra.

	Elements (in at %)		C/O ratio
	C1s	O1s	
GO	55.80	34.13	1.63
$GO_{-0.75}$	71.13	23.97	2.37
EHGO	64.14	29.99	2.14
GO-BSA	71.08	18.76	3.79

Table S-3 Fitted parameters for O1s XPS spectra.

Materials	**Parameters**	**O1s**				
		O-C=O	**C=O**	**C-OH**	**C-O-C**	chemisorbed oxygen and/or water
GO	Position (eV)	530.94	531.97	532.68	533.41	535.71
	Area	22864	19643	27373	14971	943
	percentage	26.6	23.0	31.8	17.5	1.1
EHGO	Position (eV)	530.93	531.95	532.67	533.41	535.55
	Area	20467	18612	533.41	10831	1525
	percentage	20.3	18.4	49.1	10.7	1.5
$GO_{-0.75}$	Position (eV)	530.95	531.97	532.68	533.41	535.56
	Area	10584	12952	20888	17807	1910
	percentage	16.5	20.2	32.6	27.8	2.9
GO-BSA	Position (eV)	530.94	531.94	532.67	533.41	
	Area	19981	15921	10063	3391	
	percentage	40.5	32.3	20.4	6.8	

Table S-4 Fitting parameters for GO, $GO_{-0.75}$, GO-BSA, and EHGO in the Raman spectra.

Material/Peak		GO	EHGO	$GO_{-0.75}$	BSA-GO
D*	X_c (cm^{-1})	1134	1127	1144	1167
	W (cm^{-1})	300	250	282	331
	A (%)	6	4	6	11
D	X_c (cm^{-1})	1348	1350	1347	1349
	W (cm^{-1})	144	156	150	149
	A (%)	44	48	47	37
D''	X_c (cm^{-1})	1500	1551	1488	1514
	W (cm^{-1})	169	214	116	197
	A (%)	10	16	4	16
G	X_c (cm^{-1})	1578	1565	1572	1578
	W (cm^{-1})	89	78	97	87
	A (%)	21	9	23	15
D'	X_c (cm^{-1})	1609	1603	1605	1607
	W (cm^{-1})	52	58	55	57
	A (%)	5	7	6	7
G*	X_c (cm^{-1})	2500	2569	2509	2521
	W (cm^{-1})	43	177	202	146
	A (%)	0.1	3	1	1
2D	X_c (cm^{-1})	2695	2710	2708	2669
	W (cm^{-1})	255	201	267	197
	A (%)	9	4	7	4
D+D'	X_c (cm^{-1})	2935	2904	2927	2900
	W (cm^{-1})	182	198	176	249
	A (%)	4	5	5	6
2D'	X_c (cm^{-1})	3179	3129	3156	3165
	W (cm^{-1})	154	232	167	250
	A (%)	1	3	2	2

Table S-5 Max Height intensity for some Raman peaks of GO, GO-0.75, GO-BSA, and EHGO.

Material		GO	EHGO	$GO_{-0.75}$	BSA-GO
Max Height	D*	567	463	530	967
	D	7387	6899	6927	6451
	D″	1558	2152	927	2307
	G	5475	2829	5076	4364
	D′	2789	3416	2649	2709
	G*	60	367	120	212
	2D	839	562	670	655
	D+D′	620	776	689	785
	2D′	231	329	281	250

Table S-6 Integrated area ratio for some Raman peaks of different GO.

Material	I_D/I_G	I_{D*}/I_G	A_D/A_G	$A_{D'}/A_G$
GO	1.35	0.10	2.10	0.24
EHGO	2.44	0.16	5.30	0.80
$GO_{-0.75}$	1.36	0.11	2.07	0.26
BSA-GO	1.48	0.22	2.47	0.39

Table S-7 Fitted parameters for EIS of different electrodes.

Electrodes	R1	R2	R3	W1-R	W1-T	W1-P	CPE1-T	CPE1-P	CPE2-T	CPE2-P	CPE3-T	CPE3-P
CNT/GCE	5.776	115.6		56524	1550	0.3524	5.5788E-8	0.93121	2.2198E-4	0.64281		
GO/GCE	6.535	109.5		293100	36.74	0.38336	2.3555E-8	0.97156	7.2397E-7	0.94851		
$GO_{-0.75}$/GCE	8.291	90.0		10900	0.46841	0.58	1.6648E-8	1.014	1.5696E-4	0.9		
GO-BSA/GCE	5.12	60.5	63.98	649290	11.23	0.31039	2.6731E-6	0.75595	7.8916E-7	0.9718	1.5856E-8	1.039
GO-$BSA_{-0.75}$/GCE	5.657	53.57	68.49	16249	0.45395	0.73622	9.8793E-6	0.6705	2.3443E-4	0.88004	9.544E-9	1.07
RHGO	7.87	83.74		119220	16.1	0.52752	1.4885E-8	1.025	6.0418E-7	1.16		

Table S-8 The linear range and detection limit of different electrodes.

Electrode	Linear range (μM)	Detection Limit (μM)
CNT/GCE	10-200	0.2
GO/GCE	0.2-1/1-100	0.02
$GO_{-0.75}$/GCE	0.5-20	0.5
GO-BSA/GCE	0.1-10/10-200	0.1
$GO\text{-}BSA_{-0.75}$/GCE	0.1-20	0.1
EHGO/GCE	0.5-20	0.2

Table S-9 Comparison of different modified electrodes for electrochemical detection of UA.

Electrode material	Electrochemical Method	pH	Linear range (μM)	Detection limit (μM)	Ref.
CNP	DPV	7.0	25-2500	0.2	[1]
MC-GO-Fe_3O_4	DPV	7.0	0.5-140	0.17	[2]
Ni@CNRs	DPV	7.0	0.5-30/ 35-100	0.166	[3]
CoPc/GQDs	DPV	7.0	10.76-3003	0.145	[4]
COF/La_2O_3/MWCNTS	DPV	7.0	0.4-450	0.024	[5]
g-C_3N_4/MWNTs/GO	DPV	7.0	4-200	1.36	[6]
ERGO/ZnO	DPV	7.0	1-400	0.45	[7]
GQDs	DPV	6.5	10-1000	0.107	[8]
N-rGO	DPV	7.0	1-30	0.2	[9]
GO/AuNR	DPV	7.0	10-90	0.4	[10]
Co_3O_4-ERGO	DPV	7.0	5-500	1.5	[11]
CNT	DPV	7.0	10-200	0.2	**This work**
GO-BSA	DPV	7.0	0.1-10/10-200	0.1	
GO-$BSA_{-0.75}$	DPV	7.0	0.1-20	0.1	
$GO_{-0.75}$	DPV	7.0	0.5-20	0.5	
GO	DPV	7.0	0.2-1/1-100	0.02	
EHGO	DPV	7.0	0.5-20	0.2	

1. CNP: carbon material containing nitrogen and phosphorus.[1]

2. MC-GO-Fe_3O_4: methylcellulose/graphene oxide/iron oxide nano hydrogel.[2]

3. Ni@CNRs: Nickel nanoparticles loaded with carbon nanorods.[3]

4.CoPc/GQDs: cobalt phthalocyanine anchored with graphene quantum dots.[4]

5. COF/La_2O_3/MWCNTS: covalent organic framework and lanthanum oxide and multi-wall carbon nanotubes.[5]

6.g-C_3N_4/MWNTs/GO: Graphite carbon nitride and multi-walled carbon nanotubes and Graphene oxide.[6]

7.ERGO/ZnO: Electrochemically reduced graphene oxide/zincoxide.[7]

8. GQDs: graphene quantum dots.[8]

9. N-rGO: Nitrogen-doped reduced graphene oxide.[9]

10.GO/AuNR: graphene oxide and gold nanorod.[10]

11. Co_3O_4-ERGO: Co_3O_4 nanoparticles and electrochemically reduced graphene oxide.[11]

References

1 Y. Huang, Y. Zang, S. Ruan, Y. Zhang, P. Gao, W. Yin, C. Hou, D. Huo, M. Yang and H.-b. Fa, *Microchem. J.*, 2021, 165, 106152.

2 E. Sohouli, E. M. Khosrowshahi, P. Radi, E. Naghian, M. Rahimi-Nasrabadi and F. Ahmadi, *J. Electroanal. Chem.*, 2020, 877, 114503.

3 B.-T. Liu, X.-Q. Cai, Y.-H. Luo, K. Zhu, Q.-Y. Zhang, T.-T. Hu, T.-T. Sang, C.-Y. Zhang and D.-E. Zhang, *Microchem. J.*, 2021, 171, 106823.

4 B. Wu, M. Li, R. Ramachandran, G. Niu, M. Zhang, C. Zhao, Z. Xu and F. Wang, *Adv. Mater. Interfaces*, 2023, 10, 2200738.

5 Z. Pan, H. Guo, L. Sun, B. Liu, Y. Chen, T. Zhang, M. Wang, L. Peng and W. Yang, *Colloids Surf. Physicochem. Eng. Aspects*, 2022, 635, 128083.

6 H. Wang, A. Xie, S. Li, J. Wang, K. Chen, Z. Su, N. Song and S. Luo, *Anal. Chim. Acta*, 2022, 1211, 339907.

7 M. Eryiğit, B. K. Urhan, H. Ö. Doğan, T. Ö. Özer and D. Ü, *IEEE Sens. J.*, 2022, 22, 5555-5561.

8 C. Zhao, J. Xiao, T. Liu, H. Shi, Q. Li and Z. J. I. J. E. S. Ruan, *Int. J. Electrochem. Sci.*, 2022, 17, 2.

9 A. Elangovan, K. Sudha, A. Jeevika, C. Bhuvaneshwari, P. Kalimuthu and V. Balakumar, *Colloids Surf. Physicochem. Eng. Aspects*, 2020, 602, 125050.

10 H. Safitri, W. T. Wahyuni, E. Rohaeti, M. Khalil and F. J. R. a. Marken, *RSC Adv.*, 2022, 12, 25269-25278.

11 G. Turkkan, S. Z. Bas, K. Atacan and M. Ozmen, *Anal. Methods*, 2022, 14, 67-75.